

Boosted di-boson from a mixed heavy stop

Diptimoy Ghosh^{1,*}

¹INFN, Sezione di Roma, Piazzale A. Moro 2, I-00185 Roma, Italy
and
Fermilab, P.O. Box 500, Batavia, IL 60510, USA

The lighter mass eigenstate (\tilde{t}_1) of the two top squarks, the scalar superpartners of the top quark, is extremely difficult to discover if it is almost degenerate with the lightest neutralino ($\tilde{\chi}_1^0$), the lightest and stable supersymmetric particle in the R-parity conserving supersymmetry. The current experimental bound on \tilde{t}_1 mass in this scenario stands only around 200 GeV. For such a light \tilde{t}_1 , the heavier top squark (\tilde{t}_2) can also be around the TeV scale. Moreover, the high value of the higgs (h) mass prefers the left and right handed top squarks to be highly mixed allowing the possibility of a considerable branching ratio for $\tilde{t}_2 \rightarrow \tilde{t}_1 h$ and $\tilde{t}_2 \rightarrow \tilde{t}_1 Z$. In this paper, we explore the above possibility together with the pair production of $\tilde{t}_2 \tilde{t}_2^*$ giving rise to the spectacular di-boson + missing transverse energy final state. For an approximately 1 TeV \tilde{t}_2 and a few hundred GeV \tilde{t}_1 the final state particles can be moderately boosted which encourages us to propose a novel search strategy employing the jet substructure technique to tag the boosted h and Z . The reconstruction of the h and Z momenta also allows us to construct the transverse mass M_{T2} providing an additional efficient handle to fight the backgrounds. We show that a $4-5\sigma$ signal can be observed at the 14 TeV LHC for ~ 1 TeV \tilde{t}_2 with 100 fb^{-1} integrated luminosity.

PACS numbers: 14.80.Da, 14.80.Ly, 11.30.Pb

I. INTRODUCTION

A light third generation of superpartners remains an attractive possibility to realize weak scale Supersymmetry (SUSY) [1] in nature even after the successful completion of the 8 TeV run of the Large Hadron Collider (LHC). Moreover, if a light top squark (stop) \tilde{t}_1 is the next-to-lightest SUSY particle (NLSP) just above the lightest neutralino ($\tilde{\chi}_1^0$), the lightest and stable SUSY particle (LSP) in the R-parity conserving version of the Minimally Supersymmetric Standard Model (MSSM), it would have a significant density to coexist with the LSP around the freeze-out time, and annihilations involving \tilde{t}_1 with the LSP [2] can help achieve the LSP relic density consistent with the upper bound $\Omega^{\text{DM}} h^2 < 0.128 (3\sigma)$ presented by the Planck Collaboration [3].

Such a light \tilde{t}_1 with a very small mass difference with the LSP ($\Delta m \equiv m_{\tilde{t}_1} - m_{\tilde{\chi}_1^0} \lesssim 50 \text{ GeV}$) will dominantly decay to a charm quark and the LSP [4, 5] resulting in a final state with jets and missing transverse momentum (\cancel{p}_T). Owing to the small Δm , both the charm jet and the \cancel{p}_T will be extremely soft on average making this scenario very challenging to discover experimentally [6–11].

The ATLAS collaboration has recently excluded a \tilde{t}_1 mass of 200 GeV (95% C.L.) in this channel for $\Delta m < 85 \text{ GeV}$ using 20.3 fb^{-1} of data collected at the 8 TeV run of the LHC [12]. This result clearly shows the low sensitivity of the current experimental searches to probe the degenerate stop NLSP region. Hence, it is extremely important to consider other possible signa-

tures of light third generation SUSY in the stop NLSP scenario.

Interestingly, in this region of the SUSY parameter space the heavier stop \tilde{t}_2 can also be below or around the TeV scale and it could prove useful to also look for them at the LHC. Motivated by this, we, in this paper, propose a novel search strategy to look for signatures of \tilde{t}_2 at the 14 TeV run of the LHC. Note that the signatures of \tilde{t}_2 production at the LHC has not received enough attention in the literature in the recent past primarily because of the comparatively lower cross-section (due to its heaviness) ¹. However, with a few hundred fb^{-1} integrated luminosity expected at the 14 TeV LHC, the \tilde{t}_2 production processes could be promising and can even provide information complimentary to the \tilde{t}_1 production channels.

In this paper, we consider the pair production of $\tilde{t}_2 \tilde{t}_2^*$ and their subsequent decay to either $\tilde{t}_1 Z$ or $\tilde{t}_1 h$ final states (See Fig.1). Note that, for the two above decays to have considerable branching ratios it is necessary to have adequate left-right mixing in the stop mass matrix [14, 15]. Interestingly, the large radiative corrections to the higgs mass required for the consistency with the experimental observation also prefers the left and right handed top squarks to be highly mixed. Hence, the two decay modes $\tilde{t}_2 \rightarrow \tilde{t}_1 Z$ and $\tilde{t}_2 \rightarrow \tilde{t}_1 h$ are indeed very well motivated, in particular in the context of the higgs discovery. In addition, if most of the electroweak gauginos except the LSP, and the sbottoms are rather heavy which can indeed happen in a large region of the SUSY

¹ See however, [13] where the authors considered a very low \tilde{t}_2 mass which in turn forced them to assume new F-term or D-term contributions to the higgs mass beyond the MSSM.

* diptimoy.ghosh@roma1.infn.it

parameter space, the branching ratio of \tilde{t}_2 to $\tilde{t}_1 Z$ or $\tilde{t}_1 h$ can be significant.

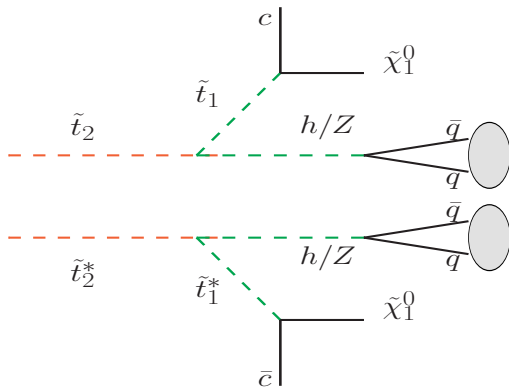


FIG. 1: Diagram showing a di-boson final state originating from $t_2 t_2^*$ pair production.

As we consider the stop NLSP scenario with a very small Δm , the \tilde{t}_1 dominantly decays via $\tilde{t}_1 \rightarrow c \tilde{\chi}_1^0$. This gives rise to a final state consisting of $hh/hZ/ZZ + \cancel{p}_T +$ very soft jets. Moreover, for an approximately TeV scale t_2 the decay products are sufficiently boosted and hence, a boosted di-boson system (h or Z) along with moderately large \cancel{p}_T is the experimental signature of such a scenario.

In the next section we will choose a couple of benchmark models where the specific decay chain mentioned above can be realized. The details of our event selection procedure will be discussed in sec.III. In sec.IV we will present the final results for our signal as well as the backgrounds and stop thereafter with some concluding remarks.

II. SUSY MASS SPECTRUM

We now briefly discuss the MSSM mass spectrum relevant for our study and present a couple a benchmark models that will be used to present our results in sec.IV. In Fig.2 we graphically show the spectrum for one of our benchmark models (Model:1) where the two conditions

1. \tilde{t}_1 is the NLSP with a small Δm ,
2. The branching ratios $\mathcal{B}(\tilde{t}_2 \rightarrow \tilde{t}_1 Z)$ and/or $\mathcal{B}(\tilde{t}_2 \rightarrow \tilde{t}_1 h)$ are significant,

can be realized.

The most important input parameters of the phenomenological MSSM (pMSSM) which can be used to reproduce such a spectrum are shown in Table-I.

Note that a low value of $\tan\beta$ and a high value of m_A are motivated from the consistency of the measured branching ratios of the rare $B_s \rightarrow \mu^+ \mu^-$ and $B_d \rightarrow X_s \gamma$ with their SM predictions. In fact, we have checked that for both the benchmark models

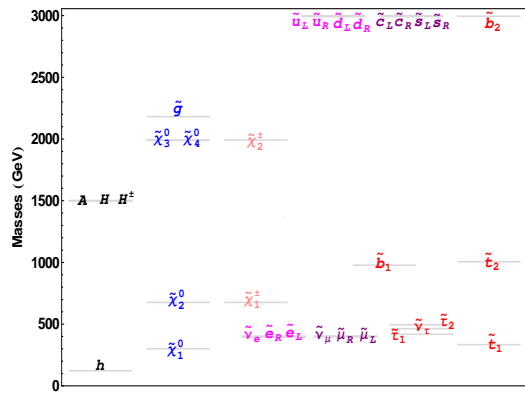


FIG. 2: Mass spectrum of the MSSM particles for our benchmark model:1.

shown in Table-I the SUSY predictions for the two above branching ratios are well inside the 2σ experimental limits [16–18]. The slepton masses are irrelevant for our discussion except the fact that the light sleptons can help ameliorate the discrepancy between the experimental measurement and the SM prediction of the anomalous magnetic moment of the muon [19, 20]. The relic density of the LSP for both the two benchmark models is also less than the Planck upper limit mentioned in the introduction. We have used the software package SuperIso Relic [21] to calculate the B -decay branching ratios, anomalous magnetic moment of muon and the dark matter relic density.

Model:1		Model:2	
pMSSM inputs	Masses	pMSSM inputs	Masses
$M_1 = 300$	$m_{\tilde{t}_2} = 1005$	$M_1 = 410$	$m_{\tilde{t}_2} = 1003$
$M_2 = 650$	$m_{\tilde{t}_1} = 334$	$M_2 = 850$	$m_{\tilde{t}_1} = 434$
$M_3 = 2100$	$m_{\tilde{\chi}_1^0} = 300$	$M_3 = 2600$	$m_{\tilde{\chi}_1^0} = 411$
$\mu = 2000$	$m_{\tilde{\chi}_2^0} = 676$	$\mu = 2000$	$m_{\tilde{\chi}_2^0} = 884$
$m_A = 1500$	$m_{\tilde{\chi}_{1\pm}} = 676$	$m_A = 1500$	$m_{\tilde{\chi}_{1\pm}} = 884$
$\tan\beta = 10$	$m_h = 123$	$\tan\beta = 7.5$	$m_h = 123$
$m_{Q3} = 1010$		$m_{Q3} = 1050$	
$m_{t_R} = 630$		$m_{t_R} = 770$	
$m_{b_R} = 3000$		$m_{b_R} = 3000$	
$A_t = -1700$		$A_t = -1600$	
$\mathcal{B}(\tilde{t}_2 \rightarrow \tilde{t}_1 Z) = 52\%$		$\mathcal{B}(\tilde{t}_2 \rightarrow \tilde{t}_1 Z) = 56\%$	
$\mathcal{B}(\tilde{t}_2 \rightarrow \tilde{t}_1 h) = 39\%$		$\mathcal{B}(\tilde{t}_2 \rightarrow \tilde{t}_1 h) = 41\%$	
$\mathcal{B}(\tilde{t}_1 \rightarrow c \tilde{\chi}_1^0) = 82\%$		$\mathcal{B}(\tilde{t}_1 \rightarrow c \tilde{\chi}_1^0) = 90\%$	

TABLE I: The relevant pMSSM input parameters, particle masses and branching ratios for our two benchmark models. The mass spectrum and the branching ratios are calculated using the public package SUSY-HIT[22].

Note that the main difference between the two models in Table-I is in the masses of \tilde{t}_1 and $\tilde{\chi}_1^0$. As the model:2 has higher values of these masses the mass gap between \tilde{t}_2 and \tilde{t}_1 is smaller which in turn makes both the \tilde{t}_1 and the Z or h less boosted.

III. COLLIDER STRATEGY

As we already mentioned in the introduction, the relevant processes of our interest are

$$\begin{aligned}
pp &\rightarrow \tilde{t}_2 \tilde{t}_2^* \rightarrow \tilde{t}_1 \tilde{t}_1^* ZZ \rightarrow ZZ \tilde{\chi}_1^0 \tilde{\chi}_1^0 c \bar{c} \\
&\quad \hookrightarrow ZZ + \cancel{p}_T + \text{soft jets} \\
pp &\rightarrow \tilde{t}_2 \tilde{t}_2^* \rightarrow \tilde{t}_1 \tilde{t}_1^* Zh \rightarrow Zh \tilde{\chi}_1^0 \tilde{\chi}_1^0 c \bar{c} \\
&\quad \hookrightarrow Zh + \cancel{p}_T + \text{soft jets} \\
pp &\rightarrow \tilde{t}_2 \tilde{t}_2^* \rightarrow \tilde{t}_1 \tilde{t}_1^* hh \rightarrow hh \tilde{\chi}_1^0 \tilde{\chi}_1^0 c \bar{c} \\
&\quad \hookrightarrow hh + \cancel{p}_T + \text{soft jets} .
\end{aligned}$$

There are several SM processes which can mimic our signal. They are all listed in Table-II. Although, two Z or higgs bosons are absent in most of the backgrounds, in practice there is always a possibility of W boson being mis-tagged as a Z or even a higgs boson. This fraction might not be very large but considering the gigantic cross sections for some of the backgrounds compared to the signal, the final contribution might not be negligible. Thus, a detailed simulation of all the background processes is necessary to make reliable predictions as we present in the next section.

As the mass gap between \tilde{t}_2 and \tilde{t}_1 is not so small in our case both the decay products of \tilde{t}_2 namely, \tilde{t}_1 and the Z or the h are expected to be moderately boosted. We thus consider the fully hadronic decays of the Z or the h in order to be able to reconstruct them using the jet substructure technique. Here we adopt the method proposed by Butterworth, Davison, Rubin and Salam (BDRS) [23] for tagging the hadronically decaying Z or the higgs boson. We briefly describe below the exact procedure used in our analysis along with our other selection criteria.

As the first step of this algorithm, we construct “fat-jets” using the Cambridge-Aachen algorithm (CA algorithm) [24] as implemented in the Fastjet package [25, 26] with R parameter of 1.0. We demand that the fat-jets satisfy $p_T > 200$ GeV and pseudo rapidity $|\eta| < 3.0$. We then take a fat-jet j and undo its last clustering step to get the two subjets j_1 and j_2 with $m_{j_1} > m_{j_2}$ by convention. The two quantities $\mu = m_{j_1}/m_j$ and $y = \Delta R_{j_1, j_2}^2 \times \min(p_{Tj_1}^2, p_{Tj_2}^2)/m_j^2$, where $\Delta R_{j_1, j_2}$ is the distance between j_1 and j_2 in the η - ϕ plane, are then computed. If there is significant mass drop i.e., $\mu < \mu_c$ and the splitting of the fat-jet j into j_1 and j_2 is fairly symmetric i.e., $y > y_c$ then we continue otherwise we redefine $j = j_1$ and perform the same set of steps as describes above on j_1 . The parameters μ_c and y_c are tunable parameters of the algorithm and are set to 0.67 and 0.10 respectively in our analysis. If the above two conditions $\mu < \mu_c$ and $y > y_c$ are satisfied then the mother jet j is taken and its constituents are re-clustered into CA jets with $R = R_{\text{filt}} = \min(\Delta R_{j_1, j_2}/2, 0.4)$ resulting in a number of jets $j_1^{\text{filt}}, j_2^{\text{filt}}, j_3^{\text{filt}}, \dots, j_n^{\text{filt}}$ ordered in descending p_T . The vector sum of the first three hardest jet momenta is then considered as the higgs candidate. The last step (the so called “filtering” procedure) is known

to captures the dominant $\mathcal{O}(\alpha_s)$ radiation from the higgs decay, while eliminating much of the contamination from underlying events [23].

Once the BDRS procedure is applied on the fat-jets, we then impose the following selection criteria on the events:

- S1 : We demand that the two hardest fat-jets (with $p_T > 200$ GeV as mentioned before) reconstruct to either a Z or a higgs boson with the mass windows [83.5-98.5] GeV and [118.5-133.5] GeV respectively.
- S2 : As our signal events have no top quark in them but most of the backgrounds do, we find it useful to veto events which have top quark in them. In order to accomplish that we again construct fat-jets out of all the stable hadrons and apply the John Hopkins top tagger (JHToptagger) [34] on them. As the top quarks in the backgrounds are mostly not highly boosted we use a comparatively large R parameter $R = 1.6$ in order to not lose most of the top quarks from the backgrounds. We set the other parameters of the JHToptagger algorithm [34] to be $\delta_p = 0.10$, $\delta_r = 0.19$, $\cos\theta_h^{\text{max}} = 0.7$ and the W mass window = (60-100) GeV. We demand the final reconstructed top mass to fall in the window (158.3-188.3) GeV. We do not demand any b-tag for the reconstruction. An event is discarded if any of the fat-jets reconstructs to a top quark by the above criteria.

As we do not also expect any hard leptons in the signal we veto events which has any lepton with $p_T > 50$ GeV and $|\eta| < 2.5$. In addition to that, we also demand that the number of normal $R = 0.4$ anti- K_T jets [35] with $p_T > 50$ GeV and $|\eta| < 2.5$ be less than 6. Note that this step kills the multi-jet background configurations e.g., $t\bar{t}$ + additional hard jets while keeping almost all the signal events.

- S3 : As \tilde{t}_2 is quite heavier than both \tilde{t}_1 and the Z or h , the \tilde{t}_1 in the decay $\tilde{t}_2 \rightarrow \tilde{t}_1 h/Z$ is expected to be rather energetic and a large part of its energy will be carried out by the LSP. Hence, even though Δm is rather small the LSP will be quite energetic to record a high \cancel{p}_T in the detectors. A strong cut $\cancel{p}_T > 400$ GeV reduces the backgrounds by a huge amount while keeping a handful of signal events.
- S4 : The charm jet from the decay of \tilde{t}_1 being very soft the topology of the decay $\tilde{t}_2 \rightarrow \tilde{t}_1 (\rightarrow c\tilde{\chi}_1^0) Z/h$ looks exactly like the one where a mother particle decays to a visible daughter particle and an invisible particle. This observation motivates us to construct the stransverse mass M_{T2} [36] out of the reconstructed Z and/or the h momenta and the missing transverse momentum. The M_{T2} constructed in this way should be distributed till the \tilde{t}_2 mass for the signal while the backgrounds are expected to populate the low mass region because there is no such heavy mother particle for the backgrounds.

Process	Production cross-section	Simulated events	No. of events after						Final cross-section (fb)	\mathcal{S} (100 fb ⁻¹)	
			S1	S2	S3	S4	S5	S6			
Signal											
Model:1	10 fb	[27]	10 ⁵	6012	4902	2736	2359	2143	1718	17.2 × 10 ⁻²	4.3
Model:2	10 fb	[27]	10 ⁵	6170	5319	2813	2421	2081	1853	18.5 × 10 ⁻²	4.6
Backgrounds											
$t\bar{t}$	833 pb	[28]	10 ⁸	221747	148580	142	41	26	11	9.1 × 10 ⁻²	
$t\bar{t}Z(1j)$	1.12 pb	[29]	226110	2484	1444	8	7	1	1	0.5 × 10 ⁻²	
$t\bar{t}W^\pm(1j)$	770 fb	[30]	276807	1365	787	5	3	3	2	0.5 × 10 ⁻²	
$t\bar{t}h(1j)$	700 fb	[31]	231064	1893	1027	2	2	2	2	0.6 × 10 ⁻²	
$t/\bar{t}W^\pm(1j)$	64 pb	[32]	6518431	7596	5801	13	9	3	3	2.9 × 10 ⁻²	
$P_1 P_2 P_3(1j)$ ($P_i \in WZh$)	500 fb	[33]	313350	1475	1093	10	5	4	2	0.3 × 10 ⁻²	
$P_1 P_2 + 1j/2j$ ($P_i \in Zh$)	5.5 pb	[33]	738779	2927	2646	3	3	3	3	2.2 × 10 ⁻²	
Total Background										16.1 × 10 ⁻²	

TABLE II: Event summary after individual selection cuts both for the SUSY benchmark points as well as the SM backgrounds. See text for more details.

Requiring a large value of M_{T2} , $M_{T2} > 400$ GeV, helps us to tame the backgrounds efficiently.

- S5 : The distribution of the effective mass of the system, $m_{\text{eff}} = \Sigma p_T(\text{hard jets and hard leptons}) + \cancel{p}_T$, being strongly correlated to $2m_{\tilde{t}_2}$ for the signal, is expected to occupy much higher mass region compared to the background. In our analysis, we require $m_{\text{eff}} > 1250$ GeV to reduce the backgrounds further.
- S6 : As the last step of our analysis we demand that there be no more than two normal jets (anti- K_T , $R = 0.4$, $p_T > 50$ GeV and $|\eta| < 2.5$ as in S2) with $\Delta R > 1.0$ with the two reconstructed Z or the h . We then also demand that none of these two jets are b-tagged. We use a 70% efficiency for b-tagging and the rate for a c-jet (light jet) mis-tagged as a b-jet to be 15% (1%) [37].

We use Pythia6.4.24[38] for generating the signal events. For most of the the backgrounds, we use Madgraph5 [33] to generate parton level events and subsequently use the Madgraph-Pythia6 interface (including matching of the matrix element hard partons and shower generated jets following the MLM prescription [39] as implemented in Madgraph5) to perform the showering and implement our event selection cuts.

IV. RESULTS AND DISCUSSION

In Table-II we show the number of signal events for our two benchmark models as well as all the backgrounds after each of the selection criteria described in the previous section has been used. In the column:10 we show the final cross section when all the selection cuts have been imposed.

Note that the number of events simulated for all the backgrounds is more than the numbers of events expected at the 14 TeV LHC with 100fb⁻¹ integrated luminosity. Thus, our estimation of the backgrounds is expected to be quite robust. In the first column the numbers within the brackets show the maximum number of additional jets which has been generated in Madgraph. For the $t\bar{t}$ background we have generated a huge number (10⁸) of events in Pythia6 (that means without additional hard jets) and checked that our background estimate agree with a smaller sample of MLM matched $t\bar{t} + \text{jets}$ events generated in Madgraph. We have also checked that the contribution of the processes $t/\bar{t}Z + \text{jets}$, $t/\bar{t}h + \text{jets}$, $W^+W^- + \text{jets}$, $W^\pm Z + \text{jets}$ and $W^\pm h + \text{jets}$ to the background is negligible.

In the ultimate column of Table-II we show the signal significance for an integrated luminosity of 100 fb⁻¹. While calculating the significance (\mathcal{S}) we use the simple recipe of \mathcal{S}/\sqrt{B} , \mathcal{S} and B being the total number of signal and background events. Any additional systematic uncertainty (which is difficult to estimate in a phenomenological study) might change the significance somewhat but will not change the conclusion of our analysis in any significant way. It can be seen that that a significance $\mathcal{S} \sim 4-5$ can be obtained with approximately 100 fb⁻¹ of data set.

In conclusion, we have considered the possibility of detecting a SUSY signal for the light stop NLSP scenario by considering the pair production of the heavier stop quark instead of the commonly considered light stop pair production channel. We have focused on the two decay channels $\tilde{t}_2 \rightarrow \tilde{t}_1 Z$ and $\tilde{t}_2 \rightarrow \tilde{t}_1 h$ giving rise to the spectacular di-boson + missing transverse energy final state. Employing the jet substructure techniques to reconstruct the hadronically decaying Z and/or higgs momenta, which also enables us to construct the M_{T2} out of the di-boson

momenta and the \cancel{p}_T , we have shown that a signal can be seen at the 14 TeV LHC with about 100 fb^{-1} integrated luminosity. It is worth mentioning at this point that there is region of MSSM parameter space where the decay $\tilde{t}_2 \rightarrow \tilde{t}_1 h$ itself can also be substantial [14] and the possibility to see even just the di-higgs signal should be investigated. This could also be important in the context of higgs self-coupling measurements which is extremely important in our endeavor to look for signatures of new physics beyond the SM.

ACKNOWLEDGMENTS

We thank JoAnne Hewett and Tom Rizzo for the hospitality at the SLAC Theory Group where this work was started. We also thank Prateek Agrawal, Wolfgang Altmannshofer, Martin Bauer, Patrick Fox, Raoul Röntsch and Felix Yu for useful discussions. The research leading to these results has received funding from the European Research Council under the European Union's Seventh Framework Programme (FP/2007-2013) / ERC Grant Agreement n.279972.

-
- [1] S. P. Martin, (1997), arXiv:hep-ph/9709356.
- [2] C. Boehm, A. Djouadi, and M. Drees, *Phys.Rev.* **D62**, 035012 (2000), arXiv:hep-ph/9911496.
- [3] Planck, P. Ade *et al.*, (2013), arXiv:1303.5076.
- [4] K. Hikasa and M. Kobayashi, *Phys.Rev.* **D36**, 724 (1987).
- [5] M. Muhlleitner and E. Popeno, *JHEP* **1104**, 095 (2011), arXiv:1102.5712.
- [6] M. Carena, A. Freitas, and C. Wagner, *JHEP* **0810**, 109 (2008), arXiv:0808.2298.
- [7] B. He, T. Li, and Q. Shafi, *JHEP* **1205**, 148 (2012), arXiv:1112.4461.
- [8] M. Drees, M. Hanussek, and J. S. Kim, *Phys.Rev.* **D86**, 035024 (2012), arXiv:1201.5714.
- [9] D. S. Alves, M. R. Buckley, P. J. Fox, J. D. Lykken, and C.-T. Yu, *Phys.Rev.* **D87**, 035016 (2013), arXiv:1205.5805.
- [10] P. Agrawal and C. Frugiuele, (2013), arXiv:1304.3068.
- [11] G. Belanger, D. Ghosh, R. Godbole, M. Guchait, and D. Sengupta, (2013), arXiv:1308.6484.
- [12] CERN Report No. ATLAS-CONF-2013-068, 2013 (unpublished).
- [13] D. Berenstein, T. Liu, and E. Perkins, (2012), arXiv:1211.4288.
- [14] G. Belanger, F. Boudjema, and K. Sridhar, *Nucl.Phys.* **B568**, 3 (2000), arXiv:hep-ph/9904348.
- [15] A. Djouadi, J. Kneur, and G. Moultaka, *Nucl.Phys.* **B569**, 53 (2000), arXiv:hep-ph/9903218.
- [16] Heavy Flavor Averaging Group, D. Asner *et al.*, (2010), arXiv:1010.1589.
- [17] LHCb collaboration, R. Aaij *et al.*, (2013), arXiv:1307.5024.
- [18] CMS Collaboration, S. Chatrchyan *et al.*, (2013), arXiv:1307.5025.
- [19] Muon G-2 Collaboration, G. Bennett *et al.*, *Phys.Rev.* **D73**, 072003 (2006), arXiv:hep-ex/0602035.
- [20] C. Gnendiger, D. Stckinger, and H. Stckinger-Kim, (2013), arXiv:1306.5546.
- [21] A. Arbey and F. Mahmoudi, *Comput.Phys.Commun.* **181**, 1277 (2010), arXiv:0906.0369.
- [22] A. Djouadi, M. Muhlleitner, and M. Spira, *Acta Phys.Polon.* **B38**, 635 (2007), arXiv:hep-ph/0609292.
- [23] J. M. Butterworth, A. R. Davison, M. Rubin, and G. P. Salam, *Phys.Rev.Lett.* **100**, 242001 (2008), arXiv:0802.2470.
- [24] Y. L. Dokshitzer, G. Leder, S. Moretti, and B. Webber, *JHEP* **9708**, 001 (1997), arXiv:hep-ph/9707323.
- [25] M. Cacciari and G. P. Salam, *Phys.Lett.* **B641**, 57 (2006), arXiv:hep-ph/0512210.
- [26] M. Cacciari, G. P. Salam, and G. Soyez, *Eur.Phys.J.* **C72**, 1896 (2012), arXiv:1111.6097.
- [27] W. Beenakker, R. Hopker, and M. Spira, (1996), arXiv:hep-ph/9611232.
- [28] M. Aliev *et al.*, *Comput.Phys.Commun.* **182**, 1034 (2011), arXiv:1007.1327.
- [29] A. Kardos, Z. Trocsanyi, and C. Papadopoulos, *Phys.Rev.* **D85**, 054015 (2012), arXiv:1111.0610.
- [30] J. M. Campbell and R. K. Ellis, *JHEP* **1207**, 052 (2012), arXiv:1204.5678.
- [31] S. Dawson, C. Jackson, L. Orr, L. Reina, and D. Wackerroth, *Phys.Rev.* **D68**, 034022 (2003), arXiv:hep-ph/0305087.
- [32] J. M. Campbell and F. Tramontano, *Nucl.Phys.* **B726**, 109 (2005), arXiv:hep-ph/0506289.
- [33] J. Alwall, M. Herquet, F. Maltoni, O. Mattelaer, and T. Stelzer, *JHEP* **1106**, 128 (2011), arXiv:1106.0522.
- [34] D. E. Kaplan, K. Rehermann, M. D. Schwartz, and B. Tweedie, *Phys.Rev.Lett.* **101**, 142001 (2008), arXiv:0806.0848.
- [35] M. Cacciari, G. P. Salam, and G. Soyez, *JHEP* **0804**, 063 (2008), arXiv:0802.1189.
- [36] C. Lester and D. Summers, *Phys.Lett.* **B463**, 99 (1999), arXiv:hep-ph/9906349.
- [37] CERN Report No. CMS-PAS-BTV-09-001, 2009 (unpublished).
- [38] T. Sjostrand, S. Mrenna, and P. Z. Skands, *JHEP* **0605**, 026 (2006), arXiv:hep-ph/0603175.
- [39] S. Hoeche *et al.*, (2006), arXiv:hep-ph/0602031.